Analysis of Models for Extracellular Fiber Stimulation

FRANK RATTAY

Abstract—**This paper presents the mathematical basis for analysis as well as for the computer simulation of the stimulus/response characteristics of nerve or muscle fibers. The results follow from the extracellular potential along the fiber as a function of electrode geometry. The theory is of a general nature but special investigations are made on monopolar, bipolar, and ring electrodes. Stimulations with monopolar electrodes show better recruitment characteristics than ring electrodes.**

Introduction

THE analysis of the effects of electrode geometry and electrical parameters is important for many applications of functional electrostimulation. This paper is relevant for example to the recruitment characteristics of motor nerves, in the timing of nerve array response produced by cochlear implants or in unidirectional peripheral nerve stimulation which blocks spastic impulses by collision.

The stimulating electrodes cause a space and time dependent potential V_e in the medium where nerve and muscle fibers are imbedded. In previous papers, it was shown that the reaction of any unmyelinated fiber is determined by the second derivative of the extracellular potential along the fiber (d^2V_e/dx^2) whereas the activation of myelinated fibers results from the difference quotient $\Delta^2V_e/\Delta x^2$ [1], [2].

We find this result from an electrical network for the current flow across the membrane of the fiber (Fig. 1). The current flow for the nth segment of the fiber at the point marked with a full circle is caused by the voltages between the different points of the network and consists of a capacitance current, an ionic current and a current along the inside. (Symbols and units are listed in Table I.)

$$C_m \frac{d(V_{i,n} - V_{e,n})}{dt} + I_{\text{ionic},n} + G_a(V_{i,n} - V_{i,n-1}) + G_a(V_{i,n} - V_{i,n+1}) = 0. \quad (1)$$

We introduce the reduced voltages

$$V_n = V_{i,n} - V_{e,n} - V_{\text{rest}} \quad (2)$$

Manuscript received May 26, 1988; November 2, 1988.

The author is with the Technical University of Vienna, A-1040 Vienna, Austria.

IEEE Log Number 8927442.

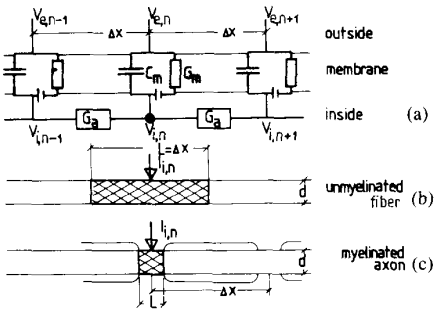

Fig. 1. Electrical network to simulate the currents in an axon. Unmyelinated as well as myelinated fibers are segmented into cylinders of length Δx. Whereas Δx is given by the internodal distance in the myelinated case, Δx depends only on computational accuracy for unmyelinated fibers. Within one segment the membrane is active in the cross-hatched area of length L which is the nodal gap width in (c), and $L = \Delta x$ in case (b). The membrane of every cylinder is simulated by an electric circuit (a) consisting of capacity C_m, an ionic voltage source, and the nonlinear membrane conductance G_m. G_a symbolizes the conductance of axoplasm between two segments. $V_{e,n}$ and $V_{i,n}$ are the external and the internal potential of the nth segment.

TABLE I
Symbols and [Units]

C_m	capacity of membrane	[μF]
c_m	capacity of membrane per cm^2	[μF/cm^2]
G_a	conductance of axoplasm	[mS/cm]
ρ_i	resistivity of axoplasm	[kΩ · cm]
ρ_e	extracellular resistivity	[kΩ · cm]
$V_{i,n}$	internal potential	[mV]
$V_{e,n}$	external potential	[mV]
V_{rest}	internal resting potential	[mV]
V_n	reduced membrane voltage (2)	[mV]
x	length coordinate of the fiber	[cm]
Δx	segmentation length of the fiber	[cm]
L	active length of membrane	[cm]
d	fiber diameter	[cm]
r	distance to electrode	[cm]
z	distance of the electrode to the fiber	[cm]
I_{el}	current of the electrode	[μA]
f	activating function (6)	[mV/cm^2]
x_j, z_j	coordinates of the jth electrode	[cm]
$I_{el,j}$	current of the jth electrode	[μA]
T	temperature	[°]
t	time	[ms]

and find

$$\frac{dV_n}{dt} = \left\{G_a(V_{n-1} - 2V_n + V_{n+1} + V_{e,n-1} - 2V_{e,n} + V_{e,n+1}) - I_{\text{ionic},n}\right\}/C_m. \quad (3)$$

By inserting $G_a = \pi d^2/4\rho_i \Delta x$ and $C_m = \pi d L c_m$ and introducing the ionic current density $i_{\text{ionic},n}$ (3) is transformed to

$$\frac{dV_n}{dt} = \left\{ \frac{d\Delta x}{4\rho_i L} \left(\frac{V_{n-1} - 2V_n + V_{n+1}}{\Delta x^2} + \frac{V_{e,n-1} - 2V_{e,n} + V_{e,n+1}}{\Delta x^2} \right) - i_{\text{ionic},n} \right\} \Big/ c_m. \tag{4}$$

The ionic currents will be described by further differential equations, e.g., the Hodgkin–Huxley equations for the unmyelinated case or the Frankenhaeuser–Huxley equations for the myelinated fiber [3], [4]. There exist several modifications of these equations and also other models are in use in order to fit them to experimental data for mammalian fibers. Of special interest is the model of Chiu *et al.* which is based on myelinated rabbit axons [5]. Their experiments showed that only sodium and leakage currents are dominant in those membranes. Sweeney *et al.* fitted their equations, which were obtained from examinations at 14°C, to warm-blooded temperature [6].

Equation (4) shows that the influence of extracellular current sources is given by

$$f_n(t) = \frac{V_{e,n-1} - 2V_{e,n} + V_{e,n+1}}{\Delta x^2} \tag{5}$$

which is the second difference quotient of the extracellular potential along the fiber. In the case of unmyelinated fibers, $L = \Delta x$ simplifies (4), and with $\Delta x \to 0$, (5) reads as

$$f(x, t) = \frac{\partial^2 V_e(x, t)}{\partial x^2} \tag{6}$$

where x is the length coordinate of the fiber.

We will call $f(x, t)$ the activating function because it is responsible for activating a fiber by extracellular stimulation. To obtain an action potential in a fiber which is at rest, the reduced voltage V_n of (2) has to become positive. Therefore, according to (4), an action potential can be generated at the fiber coordinate $x_n = n\Delta x$ if f_n is positive. In areas where f_n is negative, hyperpolarization is produced. Because $f_n(t)$ of (5) may be approximated by $f(n\Delta x, t)$ [which is the activating function of (6)] the response of myelinated and unmyelinated fibers to extracellular stimulation is quite similar qualitatively, as long as f does not vary too much within the nodal distance Δx which is in the order of 1 mm [2].

Stimulation with a Monopolar Electrode

In theory, the simplest case is the stimulation with a single monopolar spherical electrode when the ground electrode is at a distance which has no significant influence on the extracellular potential along the fiber (the distance of the fiber to the ground is more than three times the distance of the fiber to the electrode, see below). We assume a quasi-static isotropic extracellular medium

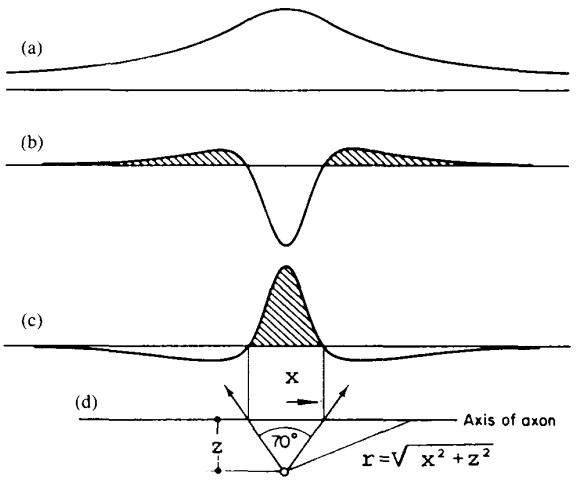

Fig. 2. Stimulation with a monopolar electrode. (a) Change of the extracellular potential along the fiber caused by anodal stimulation. Activating function for anodic (b) and cathodic (c) stimulation. (d) Shows the position of the electrode to get the upper traces. The border between depolarizing and hyperpolarizing regions is given by an angle of 70.5° and this angle does not depend on fiber parameters or the conductance of the extracellular medium [1]. Removing a negative electrode from the axon means to obtain a broader stimulating part; in the case of a myelinated axon more nodes are stimulated.

(where the biological tissue has pure ohmic resistance). The extracellular potential V_e in the distance r is given by

$$V_e = \frac{\rho_e I_{\text{el}}}{4\pi r} \tag{7}$$

where ρ_e is the extracellular resistivity and the I_{el} defines electrode current as a function of time. According to Fig. 2(d) we obtain $V_e(x, t)$ along the fiber

$$V_e = \frac{\rho_e I_{\text{el}}}{4\pi \sqrt{x^2 + z^2}} \tag{8}$$

and the activating function

$$f = \frac{\partial^2 V_e}{\partial x^2} = \frac{\rho_e I_{\text{el}}}{4\pi} (x^2 + z^2)^{-2.5} (2x^2 - z^2). \tag{9}$$

Fig. 2 illustrates the situation: the fiber will be excited in the shaded region whereas hyperpolarization is produced in those parts of the fiber where $f < 0$. The most excitable point for cathodic stimulation is $x = 0$. Strong anodic current also stimulates the fiber at two symmetrical positions according to the polarizing parts of Fig. 2(b) [2], [7]. Polarized and unpolarized regions are separated by an angle of 70° (Fig. 2) which can be calculated by setting $f = 0$ in (9).

Fig. 3 shows the reaction of an unmyelinated fiber when stimulated with a monopolar electrode. Because the subthreshold membrane resistance is nearly constant, membrane voltage along the fiber is a picture of the activating function. In the case of myelinated fibers, a snapshot shows a picture of a discrete version of f (membrane voltage is of interest only at the nodes of Ranvier) [Fig. 4].

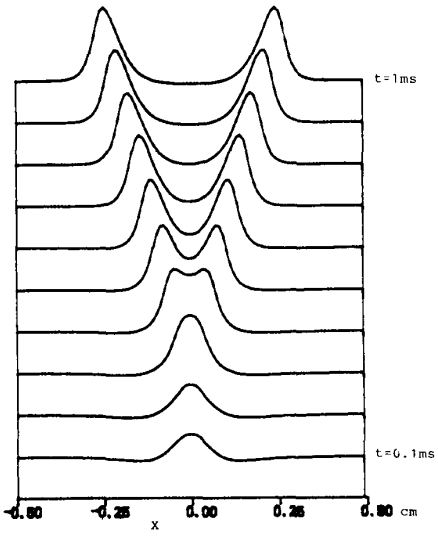

Fig. 3. Snapshots of membrane voltage along an unmyelinated axon as a response to an extracellular cathodic stimulus signal for $t = 0, 0.1, \cdots 1$ ms. At the end of a 100 μs square pulse (lowest line) the distribution of the voltage is similar to the activating function as a consequence of the nearly constant subthreshold membrane conductance. Simulation with Hodgkin-Huxley standard data, but $T = 29°C$, axon diameter 10 μm; $\rho_e = 0.3$ k$\Omega \cdot$ cm, $I_{el} = -1.5$ mA, $z = 1$ mm. Not for accuracy but for continuity in the display, 100 segments were used.

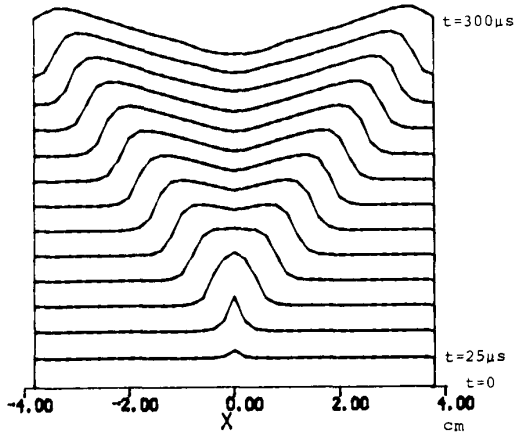

Fig. 4. Voltage distribution along a myelinated fiber at different times. 8 cm of the axon are segmented with $\Delta x = 2$ mm according to the nodal distance. The values for the membrane voltage are only defined at those discrete points which are seen by plotting weakness (points are connected by linear interpolation). The result is similar to that of Fig. 3 but high velocity is caused by myeline sheet. Simulation was done with the model used by Sweeney *et al.* [6] for 10 μm fiber diameter, nodal gap width $L = 2.5$ μm. Stimulation with a monopolar extracellular electrode located 1 mm above the node $x = 0$. Axoplasm resistivity $\rho_i = 0.055$ k$\Omega \cdot$ cm, extracellular resistivity $\rho_e = 0.3$ k$\Omega \cdot$ cm, stimulus pulse strength -30 μA, duration 0.1 ms.

The excitation of myelinated axons is very similar but different behavior appears if the electrode is very close to the fiber. If the electrode lies in the middle of two nodes and close to the axon, much higher thresholds are necessary than for electrodes just above a node [2], but this phenomenon is less important if the distance of the electrode is larger than the internodal distance. Veltink *et al.* made investigations into the statistical distribution of node positions and calculated the excitation probability for an intrafascicular point electrode as well as for an extraneural ring electrode [8].

The activating function, which is weighted according to (4) with $d\Delta x/4\rho_i L$ in the same way as the propagating voltage $\Delta^2 V/\Delta x^2$, gives only relative information on the threshold current of the electrode to reach an action potential in a certain fiber, but in order to get an absolute value we have to simulate the membrane behavior of the axon of interest. For every segment (Fig. 1) we need a subsystem of differential equations for i_{ionic} as described above. With the help of (4) and the Frankenhaeuser-Huxley equations [4] a current-distance relation can be computed which is in accordance with experimental data gathered by Ranck (Fig. 5) [7]. Electrode currents for other durations of current pulses or for other fiber diameters can be found from Fig. 6.

Other Forms of Electrodes

If several (N) monopolar electrodes with the coordinates (x_j, z_j) are in use, the corresponding activating function relative to a special fiber is defined by adding the individual influences:

$$f(x, t) = \frac{\rho_e}{4\pi} \sum_{j=1}^{N} \left[(x - x_j)^2 + z_j^2\right]^{-2.5} \cdot \left[2(x - x_j)^2 - z_j^2\right] \cdot I_{el,j}(t). \quad (10)$$

Note, that f is independent on the y coordinate, i.e., we obtain the same result for the fiber of interest if any of the electrodes rotates with the fiber as the axis.

As an example, Fig. 7 shows an estimation of the population of fibers stimulated from a dipole which lies in a plane perpendicular to a nerve. For simplicity, we assume that all fibers have the same diameter and they are stimulated by inverse current impulses at both electrodes $[I_{el,1}(t) = -I_{el,2}(t)]$. Neglecting the influence of node positions, the borders for the excited parts of the nerve may be approximated by the lines of Fig. 7 and for a special current strength all fibers will be stimulated in the shaded area.

If we also consider fibers with other diameters or if we allow statistical distribution of the nodes of Ranvier, the border between excited and nonexcited fibers is not sharp and cannot be defined by lines (for evaluations, see [8]). Such quantitative predictions on the recruitment order for special fiber distributions can be found by solving (4) together with, e.g., the Frankenhaeuser-Huxley equations. Estimations of the recruitment order according to the method used for Fig. 7 need much less computation time even we take care to the influence of fiber diameter according to Fig. 6(b). Moreover, the activating function gives basic information about the excitability of special regions. In the case of our dipole example, e.g., we see that it is not possible to stimulate fibers in the central region marked by line 0 of Fig. 7 even if current density is

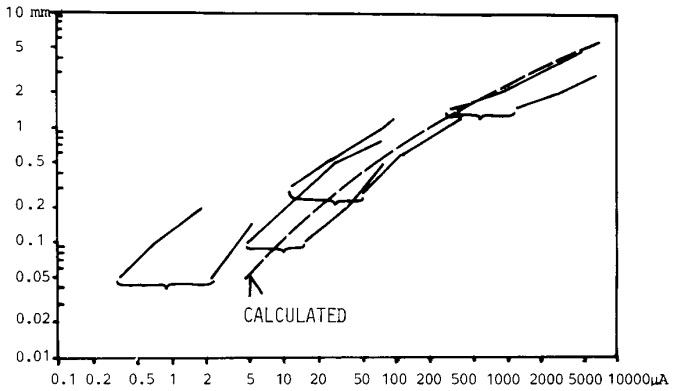

Fig. 5. Current-distance relation for monopolar cathodic stimulation of myelinated fibers. Experimental data of different authors were gathered by Ranck [7]. Their threshold currents are distributed within the left and right lines. Thresholds of experiments of the same investigators are marked with brackets. The dashed line gives the computed current-distance relation. Note that the slopes in the diagram are flatter for greater distances. The dashed line starts under an angle of 45°, this means that the electrode threshold current is proportionate to the distance of the electrode to a node (not to the fiber). For distances z in the order of 1 mm we approximately obtain a quadratic relation (doubling the distance needs four times the current). Simulation with the Frankenhaeuser-Huxley standard data, but $d = 10$ μm, $T = 37$°C, $\rho_i = 100\ \Omega \cdot$ cm, $\rho_e = 300\ \Omega \cdot$ cm. Stimulation with a 200 μs current pulse, which is also the basis for the diagram of the experiments.

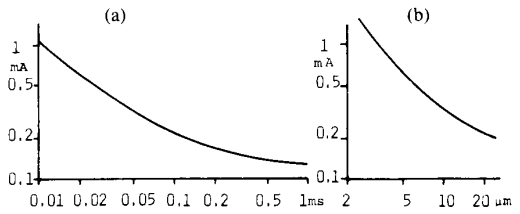

Fig. 6. Dependence of the electrode threshold current on impulse duration (a) and on axon diameter (b) for cathodic monopolar stimulation. Computed with the Frankenhaeuser-Huxley model with data as in Fig. 3, but for $z = 1$ mm. (a) $d = 20$ μm; (b) impulse duration 100 μs.

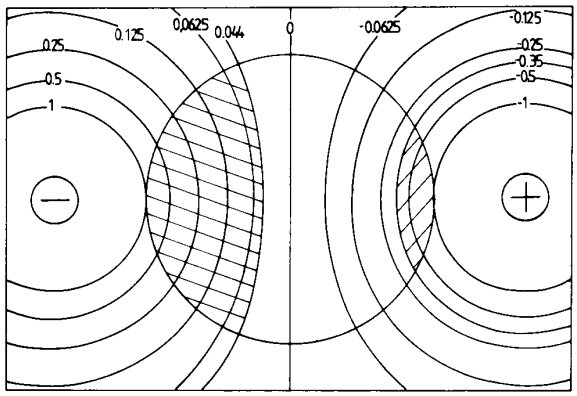

Fig. 7. Nerve stimulated by a dipole ($I_{el,-} = -I_{el,+}$). The central circle marks the boundary of a nerve which is assumed to be perpendicular to the plane of the stimulating dipole. At the lines around the poles the activating functions have the same maximum values. The numbers give the (scaled) maxima of f. Because of the broadening of the stimulating part of the axon [compare Fig. 2(d)] we need only the 8-fold current if we want to stimulate fibers at the line 0.044—compared with the most excitable fibers at line 1 at the boundary of the nerve. At the anodic part a smaller population of fibers is stimulated. Axons crossing the shaded areas will be excited. Simulation with data of Fig. 3.

high there. As the dipole lies in a plane perpendicular to the nerve, according to (10) we obtain $f(x, t) = 0$ for these axons. (The external potential of fibers crossing line 0 is zero along the whole length and the membrane will not be activated anywhere.) More generally, the use of the activating function [(10)] shows that if cathode and anode have the same x and z coordinates (relative to a special fiber) they neutralize each other ($f = 0$) independently of their relative position. This is in contrast to some older assumptions that perhaps the current densities are a measure of excitability of nerve fibers.

Fig. 8 shows the activating functions for three typical positions obtained by dipolar stimulation. The cathode is always in the same position but the anode is varied. If one electrode is about three times as far as the other, the far electrode has nearly no influence on the excitation process and the result is close to that of monopolar stimulation. By bringing the second electrode closer to the axon f becomes asymmetric. This means that one side of the axon will be activated and the other hyperpolarized. If the hyperpolarization is strong enough, the action potential will be stopped there and we get only unidirectional firing, which is of interest in certain applications. The blocking effect depends not only on the shape of the activating function in the space as well as in the time domain, but also on the recovery of the nerve membrane (Fig. 9). If

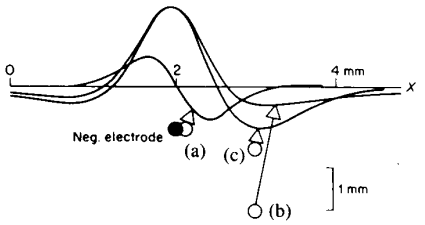

Fig. 8. Activating functions for bipolar electrodes. The cathode (full circle) is always in the same position (x = 2 mm, z = 1 mm) whereas the position of the anode is varied (a) [2.2 mm/1 mm], (b) [3 mm/3 mm] and (c) [3 mm/1.5 mm].

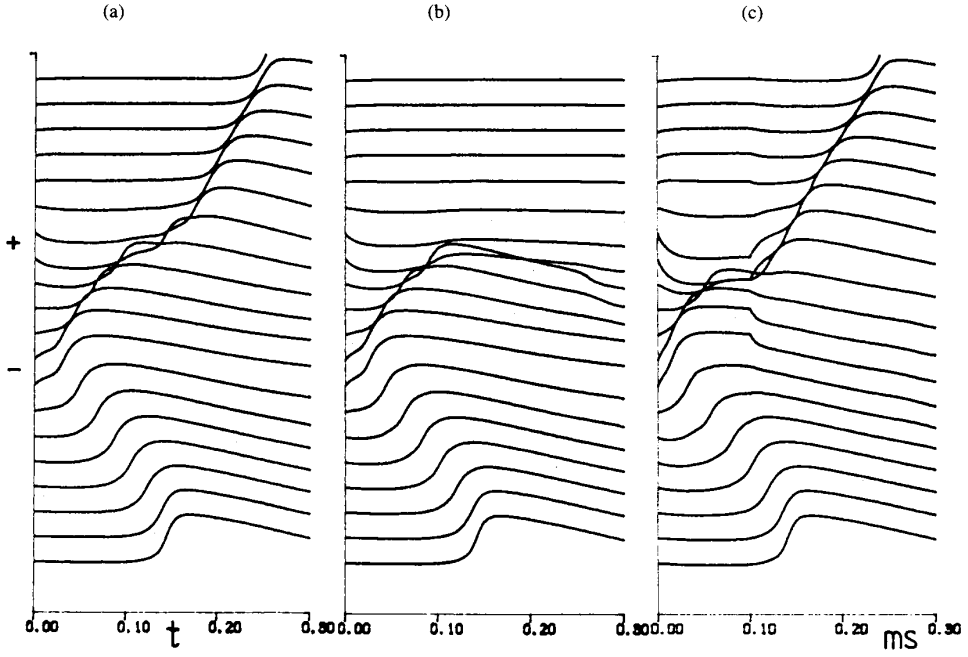

Fig. 9. Bipolar stimulation of a myelinated axon. Every line shows the membrane voltage of the axon at a node of Ranvier. Two electrodes (positions are marked − and +) are used to stimulate the fiber with inverse current impluses. In case (a) the hyperpolarization is too weak to stop the passage of the spike but stronger stimulations allow only unidirectional firing (b). In case (c) the pulse width is shorter than in (a) and because the fiber has a very short recovery time propagation of the spike is not blocked in the hyperpolarized part. Simulation was done with the model of Chiu *et al.* [5] modified according to Sweeney *et al.* [6]. Further data: internodal distance 2 mm, ρ_r = 0.3 kΩ · cm; positions of the electrodes: cathode x_{el} = 1.5 cm, z_{el} = 0.4 cm, anode x_{el} = 2.5 cm, z_{el} = 0.4 cm; electrode current 2.5 mA in (a), 3 mA in (b), and 6 mA in (c); pulse duration 300 μs in (a), (b) and 100 μs in (c).

we apply a short impulse at the dipole and if we assume that the membrane also needs only a short recovery period to leave the hyperpolarized state, it is possible that the excited part of the axon overcomes also the former hyperpolarized part and the action potential propagates to both directions.

Ring electrodes as well as other types of implanted electrodes can be approximated by a number of single electrodes. By means of (10) the corresponding activating functions are calculable. As an example, we will compare the nerve excitation by monopolar and by ring electrodes. Fig. 10 shows the small difference in the activating functions obtained for one of the most excitable points at the edge of the nerve and for the point in the center, which is most difficult to excite. The small variation of f gives the reason for the bad recruitment order obtained from exper-

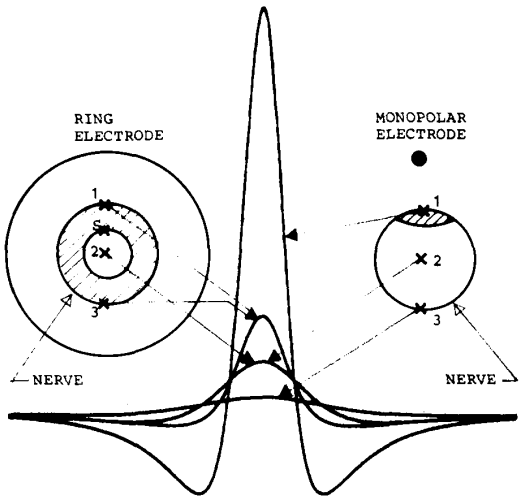

Fig. 10. Activating functions for ring electrodes and for monopolar electrodes. The activating functions for three different fibers in a nerve are marked by triangles. In the case of stimulation with a ring electrode the situation is axial symmetric and case 1 and 3 give the same result. The central fiber 2 is hardest to stimulate, but because the maximum of the activating function for this position is not considerably smaller than for fibers at the edge (1, 3) ring electrodes have bad recruitment characteristics. Monopolar electrodes show much more variations in the amplitude of f. If the same current signal is applied at both types of electrodes we obtain exactly the same f for the central fiber 2. For a point S in the middle of position 1 and 2, in the case of the ring electrode, the amplitude of f is 61 percent of the amplitude of the activation function of position 1. If we assume that I_{el} brings a fiber at S to threshold, all fibers with the same or greater diameter lying in the shaded area (which is 75 percent of the total nerve area) will fire, too. In the case of a monopolar electrode the same situation ($f_{max,S} = 0.61 \cdot f_{max,1}$) excite a much smaller population of fibers (shaded area). The radius of ring electrode was assumed to be twice the radius of nerve and the same as the distance of the monopolar electrode to the central fiber (position 2).

iments as well as from other calculations. Much better results are obtained by the theory for the stimulation with a monopolar electrode as demonstrated by Fig. 10.

Discussion

We have made many simplifications in order to get a simple model. For special applications, the theory should also take into consideration inhomogenity and anisotropy of the extracellular medium, deviation from pure ohmic resistance in the extracellular medium, fatigue and statistical influences, and changes of firing behavior if a great part of fibers in a nerve are stimulated simultaneously.

We were not concerned in this paper with the calculation of the extracellular potential for complicated geometries. In the vicinity of surface electrodes we can estimate the activating function by analytical methods [9]. With finite differences or finite element methods we are able to estimate the activating functions also for complicated forms of electrodes and as a function of body geometry. Several investigators have used finite differences or finite element methods to find potential distributions or current density distributions for special parts of the body, but with few exceptions it was not recognized that the activating function (or at least the extracellular potential together with the network of Fig. 1) should be calculated in order to predict nerve behavior. In this paper we were mostly concerned with estimations of the recruitment order which is of special interest for motor nerve stimulation. It was shown that ring electrodes are not suited for adjusting and monopolar electrodes have better characteristics [2], [7], [8], [10].

Using cochlear implants it is also very important to get different firing behavior in the axons of the auditory nerve. Monopolar electrodes show here good recruitment characteristics because the difference between just perceptible and uncomfortable loudness is obtained when electrode currents reach about six times the threshold value. Several investigators separate the frequencies of the acoustic source signal and provide different channels simultaneously with stimulus signals. Unfortunately, the stimulating signals interact and by simulation [using (4) and (10)] it can be shown that the firing frequency of a special fiber is not only determined by the closest pair of electrodes. This may be a reason that single channel stimulation reaches similar quality of perception as multichannel techniques. In order to avoid confusion by multichannel interferences, the author has presented a single channel strategy which supports more graduated nerve array responses [11].

The theory should find further applications in unidirectional firing techniques. In order to find the activating functions for special forms of electrodes computer simulations are still being made and they will help designing optimal electrode geometries [12]. Unfortunately, there is still a lack of usable models for ionic currents which define membrane behavior.

References

[1] F. Rattay, "Analysis of models for external stimulation of axons," *IEEE Trans. Biomed. Eng.*, vol. BME-33, pp. 974–977, 1986.
[2] —, "Ways to approximate current-distance relations for electrically stimulated fibers," *J. Theor. Biol.*, vol. 125, pp. 339–349, 1987.
[3] A. L. Hodgkin and A. L. Huxley, "A quantitative description of membrane current and its application to conduction and excitation in nerve," *J. Physiol. (London)*, vol. 117, pp. 500–544, 1952.
[4] B. Frankenhaeuser and A. F. Huxley, "The action potential in the myelinated nerve fiber of Xenopus Laevis as computed on the basis of voltage clamp data," *J. Physiol. (London)*, vol. 171, pp. 302–315, 1964.
[5] S. Y. Chiu, J. M. Ritchie, R. B. Roggart, and D. Stagg, "A quantitative description of membrane currents in rabbit myelinated nerve," *J. Physiol. (London)*, vol. 292, pp. 149–166, 1979.
[6] J. D. Sweeney, J. T. Mortimer, and D. Durand, "Modeling of mammalian myelinated nerve for functional neuromuscular stimulation," presented at IEEE/Ninth Annu. Conf. Eng. Med. Biol. Soc., Boston, MA, 1987, pp. 1577–1578.
[7] J. B. Ranck, Jr., "Which elements are excited in electrical stimulation of mammalian central nervous system: A review," *Brain Res.*, vol. 98, pp. 417–440, 1975.
[8] P. H. Veltink, J. A. van Alste, and H. B. K. Boom, "Simulation of intrafascicular and extraneural nerve stimulation," *IEEE Trans. Biomed. Eng.*, vol. BME-35, pp. 69–75, 1988.

[9] F. Rattay, "Modeling the excitation of fibers under surface electrodes," *IEEE Trans. Biomed. Eng.*, vol. BME-35, pp. 199-202, 1988.
[10] P. G. Gorman and J. T. Mortimer, "The effect of stimulus parameters on the recruitment characteristics of direct nerve stimulation," *IEEE Trans. Biomed. Eng.*, vol. BME-30, pp. 407-414, 1983.
[11] H. Motz and F. Rattay, "Signal processing strategies for electrostimulated ear prostheses based on simulated nerve response," *Perception*, vol. 16, pp. 777-784, 1987.
[12] A. S. Ferguson, J. D. Sweeney, D. Durand, and J. T. Mortimer, "Finite difference modeling of nerve cuff electric fields," presented at IEEE/Ninth Annu. Conf. Eng. Med. Biol. Soc., Boston, MA, 1987, pp. 1579-1580.

Frank Rattay was born in Tyrol, Austria, on May 29, 1945. He studied geodesy and technical mathematics and received the Dipl. Ing., Dr. techn., and Habilitation degrees from the Technical University of Vienna, Vienna, Austria, in 1974, 1980, and 1987, respectively.

Since 1972 he has been with the Institute of Analysis, Technische Mathematik und Versicherungsmathematik of the Technical University of Vienna. His main scientific interests include electrostimulation, hearing theory and speech features. Additionally, he has served as a consulting engineer for projects in underdeveloped countries.